Facilitating the Development of a Novel Heavy-Duty Offroad Vehicle Exploiting Hardware-in-the-Loop Technique

Weijin Qiu [1], Shubham Ashta [1], Gregory M. Shaver [1], Scott Johnson [2], Bryan C. Frushour [3]

[1] Ray W. Herrick Laboratories, Mechanical Engineering, Purdue University, West Lafayette, IN, USA 47907

[2] John Deere Intelligent Solutions Group, Fargo, ND, USA 58102

[3] John Deere Electric Powertrain, Waterloo, IA, USA50701

Abstract

Stricter emissions regulations have placed unprecedented pressure on off-road OEM companies to reduce the fuel consumption of their products. This has led to the adoption of powertrain electrification as a viable solution. The increased complexity associated with powertrain electrification necessitates a more reliable and efficient testing approach to assess the control performance of off-road vehicles with electrified powertrains. In this study, a real-time hardware-in-the-loop (HIL) simulation platform was developed for validating a novel heuristics-based vehicle power management (VPM) strategy to be implemented on a novel heavy-duty offroad wheel loader featuring battery-hybrid powertrain configuration. The platform incorporates a vehicle power management strategy for power distribution, component-level controllers to oversee actuator functions, and physics-based models of powertrain components to mimic vehicle performance. This HIL simulation platform enables the safe and efficient testing and validation of a controller board comprising the VPM strategy and a DC/DC converter control system. Results from simulations conducted on the HIL platform demonstrate that the studied battery hybrid wheel loader can achieve over 10% fuel savings.

Keywords. Off-road vehicles, vehicle power management, hybrid vehicles, hardware-in-the-loop simulation.

1. INTRODUCTION

Electrifying off-road vehicles is necessary to address critical environmental and operational challenges facing the industrial and agricultural sectors. By transitioning to electric powertrains, off-road vehicles can significantly reduce harmful emissions, contributing to improved air quality and reduced environmental impact. Furthermore, electrification offers the potential to enhance operational efficiency, lower operating costs, and mitigate the reliance on fossil fuels, thereby promoting sustainability and resource conservation. The shift towards electrification also aligns with evolving regulatory standards and societal expectations regarding carbon emissions and environmental stewardship. Additionally, electric powertrains can provide off-road vehicles with improved torque characteristics, precise power delivery, and quieter operation, enhancing overall performance and operator comfort. Embracing electrification in off-road vehicles represents a crucial step towards building a cleaner, more sustainable future for industrial and agricultural machinery, ensuring a healthier environment and more efficient operations for years to come [1].

As one of the largest manufacturing corporations in the US, John Deere introduced its first production electric wheel loader, the 644k, in 2012, wherein its powertrain was transitioned from a conventional transaxle with a hydraulic torque converter to a series electric powertrain without an energy storage system. This very first evolution of this type of machine reduced its engine size from 9.0 L to 6.8 L, and provided a 30% gain in fuel efficiency. The presented work is part of a research effort aiming at developing a battery-hybrid wheel loader for John Deere based upon this production 644k series electric wheel loader by furthering downsizing the engine and adding an electric energy storage system. Note that the incorporation of a battery requires a vehicle power management (VPM) to regulate the power flows between power sources and power consuming units, which raises the demand for appropriate simulation tools to test its algorithm rapidly and safely before being implemented on a demo vehicle for in-field testing.

Hardware-in-the-loop (HIL) testing is a method utilized for controller validation, involving the interaction of actuating signals from an actual controller with a test rig that replicates real-world physical systems to simulate the

controller's performance in an assembled product. One significant advantage of utilizing this method is its ability to notably reduce the cost, time, and safety risks associated with controller development, verification, and debugging [2]. Given the characteristics of HIL testing, it is well-suited for validating the VPM strategy proposed in this study. As there is limited existing literature on the establishment of a comprehensive hardware-in-the-loop simulation platform for the hybrid electric wheel loader application, the content presented in this paper would partially address this gap.

2. SYSTEM MODELING & CONTROL DEVELOPMENT

2.1. Powertrain

Fig. 1 showcases the configuration of the baseline wheel loader examined in this research. A 6.8 L diesel engine is linked to a generator motor and a hydraulic pump responsible for bucket operations via a planetary gearbox. The generator motor, powered by the engine, generates AC power, which is subsequently transformed into DC power by a rectifier. For simplicity, a DC-link between the rectifier and the inverter has been omitted. When the generator motor supplies electricity, the inverter has the capability to extract direct currents from the DC-link and convert them back into alternative currents to drive the electric motor for vehicle propulsion.

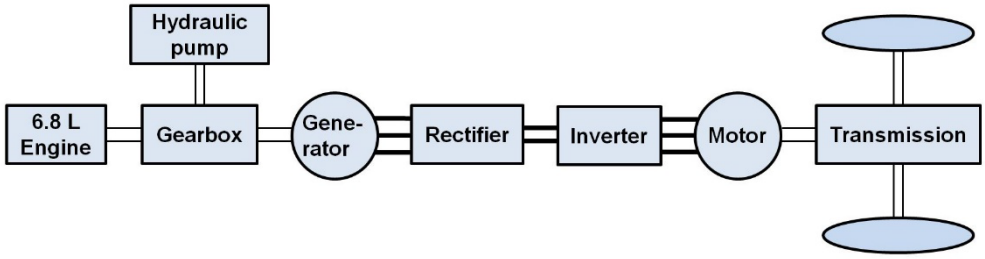

Figure 1. Baseline powertrain architecture

The powertrain of the envisioned wheel loader depicted in Figure 2 undergoes a transformation from this arrangement by reducing the engine size from 6.8 L to 4.5 L and integrating a battery pack to compensate for the diminished torque and power capability resulting from the engine reduction. Additionally, an electrically-driven pressure charging device, known as an "eBooster," is introduced to enhance boost pressure and transient engine performance.

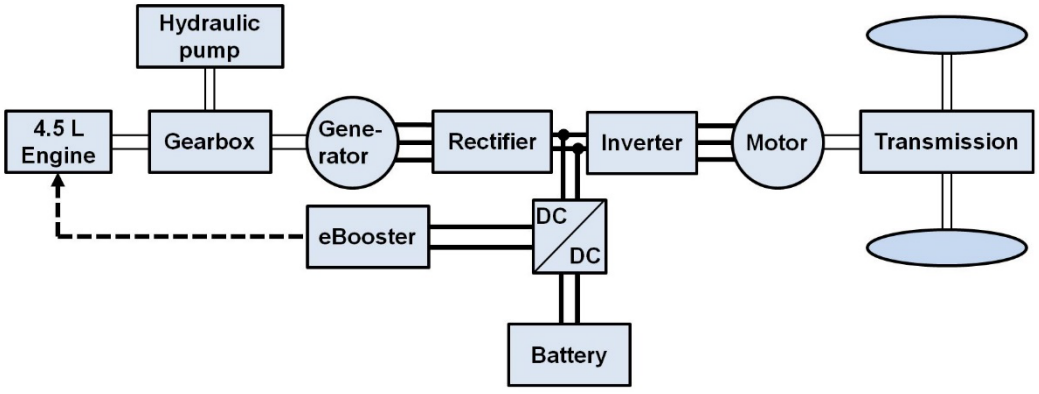

Figure 2. Proposed powertrain architecture

2.2. Engine

The 4.5 L turbocharged diesel engine, utilized as one of the two primary power sources for the proposed wheel loader, is integrated into the architecture illustrated in Fig 3. To model the engine's performance and fuel

consumption, a state-space form nonlinear engine model can be developed based on fundamental principles [3, 4]. It is important to acknowledge that, for the sake of simplicity in the model, the dynamics of the eBooster were omitted, although the engine's torque and power properties have accounted for the influence of the eBooster.

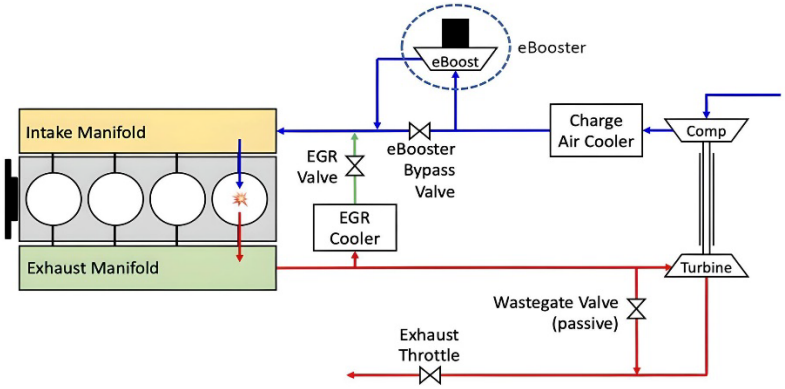

Figure 3. Engine schematic

Determining the actual engine speed involves conducting a torque balance analysis on the crankshaft [5] of the engine under investigation, resulting in:

$$\frac{d\omega_{eng,act}}{dt} = \frac{1}{J_{eng}}(T_{ind} - T_{hyd} - T_{gm}) \tag{1}$$

In the expression above, J_{eng} denotes moment of inertia of the engine crankshaft. T_{ind}, T_{hyd}, and T_{gm} represents indicated torque, load torque applied by the hydraulic system, and load torque applied by the generator motor, respectively. The indicated torque T_{ind} is a controller output generated by a production engine speed controller in PI form.

Furthermore, engine fuel consumption can be calculated as shown below per [6]:

$$\dot{M}_{fuel} = \frac{\omega_{eng,act} T_{ind}}{\eta_{therm} Q_{LHV}} \tag{2}$$

In the above expression, Q_{LHV} stands for gas lower heating value of diesel fuel, which is treated as a constant. η_{therm} denotes brake thermal efficiency and can be modeled as a function of actual engine speed and air-fuel ratio (AFR) [7]. Fig. 4 demonstrates an illustrative diagram of the engine model and control strategy deployed in this study.

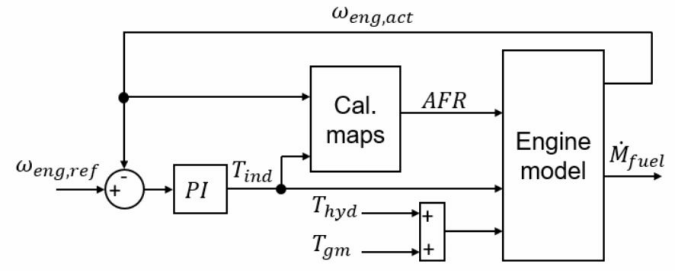

Figure 4. Engine model & control diagram

2.3. Battery

The battery model employed in this study is relatively straightforward, aiming primarily to forecast the state-of-charge (SOC) of the battery at any given moment and the system voltage of the battery. This study utilizes the Coulomb counting method to compute the battery SOC, which necessitates the input of battery current and initial battery SOC to proceed. Here, C represents the battery capacity, and $I(t)$ denotes the battery current.

$$SOC(t) = SOC(t_0) + \frac{1}{C}\int_{t_0}^{t} I(t)dt \tag{3}$$

The system voltage of the battery can be acquired by referencing a specification data sheet supplied by the battery manufacturer, which establishes a correlation between battery SOC and system voltage. Additionally, the specification data sheet from the battery manufacturer includes current restrictions for charging and discharging based on battery SOC, represented as $I_{chg,max}$ and $I_{dis,max}$, respectively. Fig. 5 depicts an illustrative diagram for the battery model.

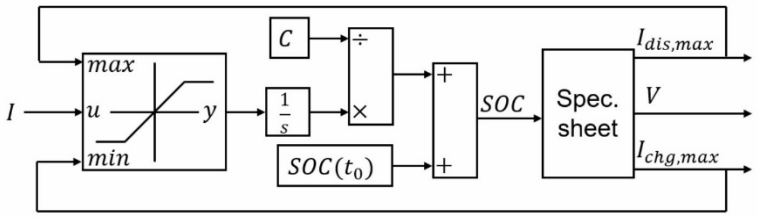

Figure 5. Battery model diagram

Table 1 presents essential specifications of the acquired battery pack utilized to establish the battery model. It is worth noting that the maximum discharge C-rate of the battery is 5 C, equating to a maximum discharge power of 177.5 kW. The battery is not designed for operation at this power level for more than 10 seconds; hence, this maximum discharge C-rate is labelled as "pulse." Conversely, the maximum continuous discharge C-rate of the battery is 3 C, corresponding to a discharge power of 106.5 kW. Temperature represents another crucial factor influencing battery properties. For the purposes of this study, it is assumed that the battery and thermal management systems can maintain the battery temperature at approximately 300 K.

Table 1. Specifications of sourced battery

Specification	Value
Nominal voltage	355 V
Min/Max voltage	288 V/403 V
Rated capacity	100 Ah
Rated energy	35.5 kWh
Max discharge C-rate (pulse)	5 C
Max discharge C-rate (continuous)	3 C
Max charge C-rate	2 C

2.4. Power Electronics

The power electronics components examined in this study encompass a generator motor and its associated controlling rectifier, a traction motor and its corresponding controlling inverter, and a DC/DC converter for battery management. To replicate their behaviors during operation within the vehicle under investigation, an electrical circuit for this power electronics system is formulated using the eHS solver, which is a real-time power electronics

simulation solver that facilitates simulation of an electric circuit on a FPGA, without needing to write mathematical equations. Fig. 6 displays a visual representation of the created electrical circuit.

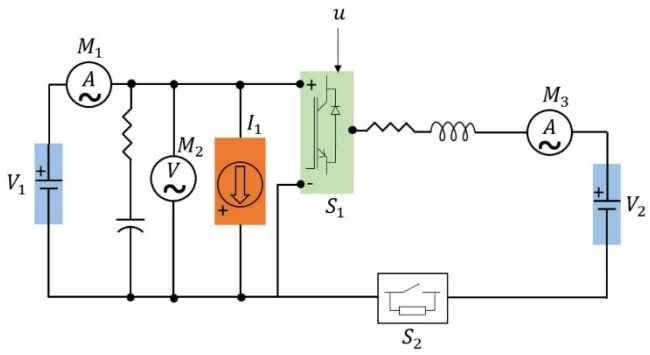

Figure 6. Illustrative layout of designed electrical circuit

Within the circuit, an ideal voltage source V_1 is utilized to simulate the generator and its corresponding bidirectional rectifier, as the rectifier is configured to operate in voltage control mode for the proposed hybrid vehicle design. During the operation of the proposed hybrid vehicle, any activity involving the traction motor or the battery, whether it entails power consumption or power supply, leads to fluctuations in the DC-link voltage, reflecting a power imbalance. By configuring the rectifier in voltage control mode, the generator is prompted to provide or absorb an appropriate amount of electrical power to or from the DC-link, thereby compensating for the power imbalance. The ideal voltage source is adjusted to supply a constant 700 V voltage. Typically, the generator supplies electrical power to the DC-link, resulting in the imposition of an electromagnetic load torque on the engine, denoted by the term T_{gm} in Eq. 1. To model this electromagnetic load torque, the current supplied by the generator I_{gm} and the DC-link voltage V_{dc} are measured, for which a current sensor M_1 and a voltage sensor M_2 are incorporated into the circuit, respectively. This load torque can then be formulated as demonstrated in Eq. 4, where η_{gm} represents the generator motor efficiency, and r signifies the gear ratio between the engine and the generator, and is utilized for further simulation purposes.

$$T_{gm} = \frac{I_{gm} V_{dc} \eta_{gm}}{\omega_{eng} r} \tag{4}$$

To model the traction motor and its associated bidirectional inverter, an ideal current source labelled as I_1 is utilized within the circuit. This approach is adopted to simulate two specific scenarios: vehicle propulsion, during which the traction motor draws current from the DC-link, and vehicle braking, where the traction motor injects current into the DC-link. The magnitude of the current passing through this ideal current source I_{tm} is contingent upon the power required by the operator for propulsion or braking P_{tm}, and the efficiency of the traction motor η_{tm}, as outlined below.

$$I_{tm} = \frac{P_{tm} \eta_{tm}}{V_{dc}} \tag{5}$$

The accuracy of the DC/DC converter model for battery control in this study, denoted as S_1 in the circuit, surpasses that of the other power electronics models, as it is intended to validate an actual controller governing battery current during simulation. Therefore, the fidelity of its model was increased and Fig. 7 presents a more intricate layout of the converter model.

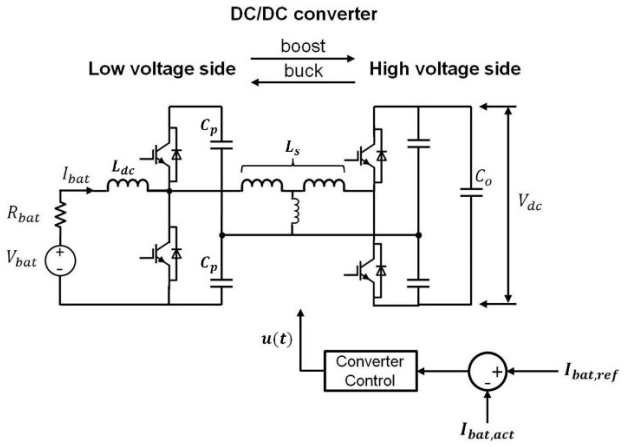

Figure 7. Illustrative layout of converter model

The proposed hybrid vehicle necessitates a high-power bidirectional DC/DC converter to interface with the vehicle's battery, given the substantial voltage differential between the 700 V DC-link (high voltage side, HVS) and the battery, which has a nominal voltage of 350 V (low voltage side, LVS). When power transfers from the battery to the DC-link, the DC/DC converter operates as a boost converter. Conversely, when the power flow direction is reversed, the DC/DC converter functions as a buck converter. The magnitude and direction of power flow between the battery and DC-link are regulated by a converter controller, which operates as a PI controller in current control mode. The input to the converter controller constitutes the error between the reference battery current and the actual battery current, compelling the converter controller to respond and generate appropriate gating signals $u(t)$ to achieve an instantaneous desired phase angle shift between LVS and HVS voltages. This is accomplished by a specific gating pattern, assuming a constant drive cycle and switching frequency. Ultimately, this phase angle shift ϕ, as depicted in the equation below, aligns the actual battery current with the reference battery current, where ω denotes the converter's switching frequency.

$$\frac{dI_{bat}}{dt} = \frac{\int \left(\frac{I_{bat}}{2C_p} - \frac{\phi(\pi-\phi)V_{dc}}{2C_p\omega L_s}\right) dt + V_{bat} - I_{bat}R_{bat}}{L_{dc}} \tag{6}$$

To verify the DC/DC converter's ability to effectively monitor battery current, a current sensor M_3 is integrated into the circuit to compare its measurement with the corresponding reference value. Additionally, another ideal voltage source, denoted as V_2, is introduced to simulate the battery voltage and complete the circuit, with the voltage value derived from the previously described battery model.

3. VEHICLE POWER MANAGEMENT

For certain component-level controllers to operate effectively, a supervisory-level vehicle power management (VPM) strategy must provide the necessary reference signals. At the system level, this VPM strategy governs the regulation of power flows within the vehicle by generating directives for the component-level controllers to execute. The control architecture of the proposed hybrid vehicle is depicted in Fig. 8. Notably, the control variables derived from the power management strategy chosen for this hybrid vehicle consist of the commanded engine speed ω_{eng} for the engine controller, the commanded battery current I_{bat} for the converter controller, and the available torque limit $T_{tm,max}$ for the inverter controller.

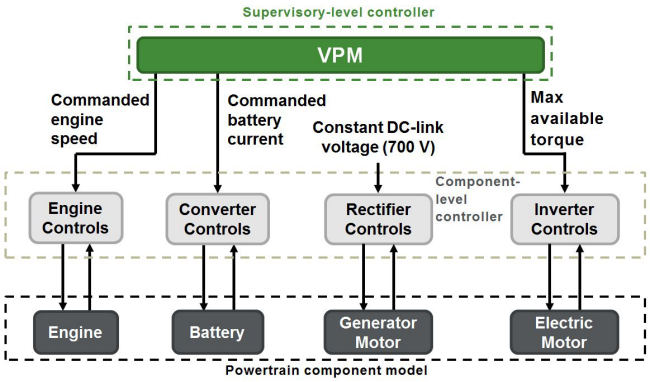

Figure 8. Control architecture of the battery-hybrid vehicle

Fundamentally, the developed VPM strategy for this research should have the ability to distribute the power demanded by the operator from multiple power sources to various power-consuming units of the proposed vehicle (within physical constraints), optimize engine operation for maximum efficiency, and manage battery operation to maintain battery state of charge (SOC). Fig. 9 illustrates the heuristic-based algorithm of the designed VPM strategy for calculating the commanded engine power $P_{eng,cmd}$ and the commanded battery current $I_{bat,cmd}$. In the algorithm, $P_{hyd,req}$, $P_{trac,req}$, and $P_{load,para}$, represent the hydraulic power requested by the operator, the traction power requested by the operator, and the auxiliary load power estimated by the vehicle's transmission control unit (TCU), respectively. It is noteworthy that these requested power terms are predominantly positive, although $P_{trac,req}$ may be negative during energy regeneration. Additionally, $P_{bat,max}$, $P_{bat,min}$, $P_{dis,max}$, and $P_{chg,max}$ can be defined as follows:

$$
\begin{aligned}
P_{dis,max} &= I_{dis,max} V_{bat} \\
P_{chg,max} &= I_{chg,max} V_{bat} \\
P_{bat,max} &= \begin{cases} P_{dis,max}, SOC_{act} > SOC_{ref} \\ P_{SOC}, SOC_{act} < SOC_{ref} \end{cases} \\
P_{bat,min} &= \begin{cases} P_{SOC}, SOC_{act} > SOC_{ref} \\ P_{chg,max}, SOC_{act} < SOC_{ref} \end{cases}
\end{aligned} \tag{7}
$$

In the above equation, P_{SOC} is defined as a tuneable control limit of the battery in the format of a PI controller, with the differential value between target SOC SOC_{ref} and actual SOC SOC_{act} being the controller input, and battery power control limit P_{SOC} being the controller output.

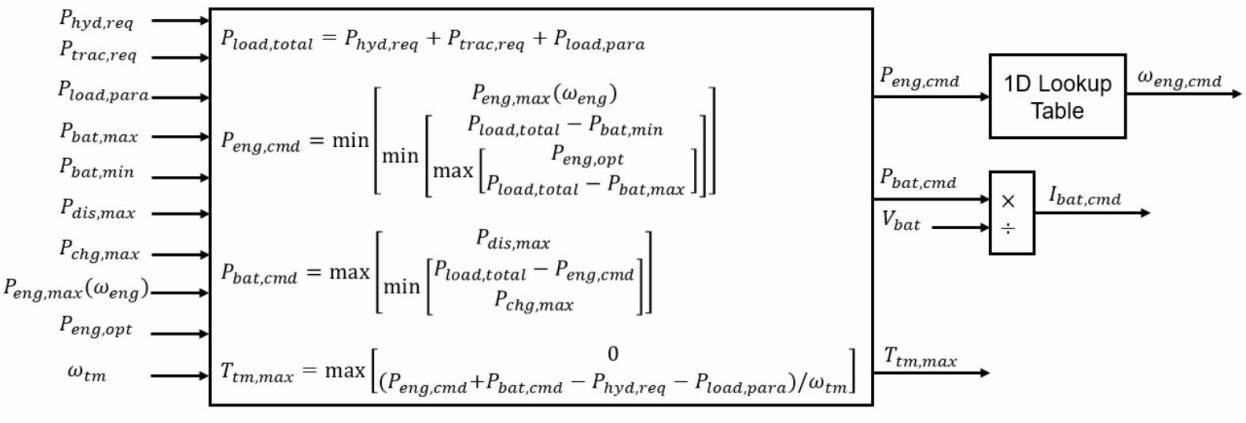

Figure 9. Vehicle power management strategy

Additional terms requiring clarification in the algorithm include the maximum engine power $P_{eng,max}$ at the current engine speed, the optimal engine power $P_{eng,opt}$ indicating the power level at which the engine achieves the lowest brake specific fuel consumption (BSFC) value, and the traction motor speed ω_{tm}.

After determining the commanded engine power $P_{eng,cmd}$, the VPM strategy will choose a commanded engine speed based on the engine efficiency map. This selected engine speed aims to achieve the best fuel economy while operating at the specified power level. Nevertheless, the chosen engine speed may be constrained by various factors, such as the operational speed limit of the hydraulic pump [8], leading to a suboptimal engine speed as the ultimate result.

Through the generation of a commanded engine power $P_{eng,cmd}$ and commanded battery current $I_{bat,cmd}$, the VPM strategy can compute the available power limit for the electric motor with the aid of the TCU. This calculated value is then transformed into a maximum torque value that the electric motor can deliver for vehicle propulsion, serving as the third output. Further detailed explanation about this algorithm can be found in [9].

4. HAREDWARE-IN-THE-LOOP TESTING

4.1. Experimental Setup

In this research, a novel HIL simulation platform has been established, and Fig.10 displays an actual image of the deployed HIL simulator. To provide a clearer depiction of its structure and the interactions between each element, Fig.11 illustrates a layout of the platform. This simulation platform comprises four main components: a physical controller board housing the designed VPM strategy and a converter controller for the battery, which serves as the "hardware" under examination in this system; an FPGA module utilized for executing the eHS solver to simulate the power electronics employed in this study; a CPU module responsible for executing the plant model; and a host PC used as a console and monitor.

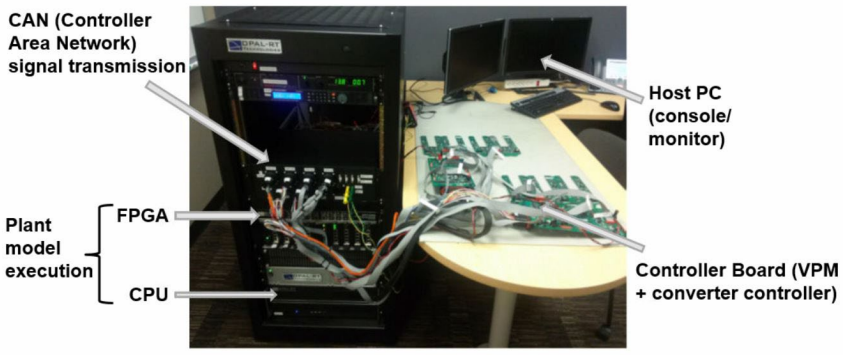

Figure 10. Image of the deployed HIL simulator

By employing the innovative HIL simulation platform, the following three objectives can be safely and efficiently accomplished: (1) executing the VPM strategy on actual hardware in real time to evaluate its functionality, specifically its ability to operate in real time on a vehicle implementable controller board and communication bus; (2) validating the converter controller's capacity to regulate battery current; (3) evaluating the potential fuel savings of the proposed battery hybrid electric wheel loader in comparison to the baseline wheel loader. To enable a valid comparison between the baseline vehicle and the proposed vehicle, a typical production drive cycle of the baseline wheel loader known as "Stockpile" is replicated in the HIL simulation platform for the proposed wheel loader. This is achieved by inputting the experimental load (power) data obtained from an actual baseline wheel loader running the "Stockpile" drive cycle into the HIL simulation platform via the host PC, prompting the platform to simulate vehicle performance. The simulation results of the proposed vehicle can then be compared to the experimental results of the baseline vehicle for validation and assessment purposes.

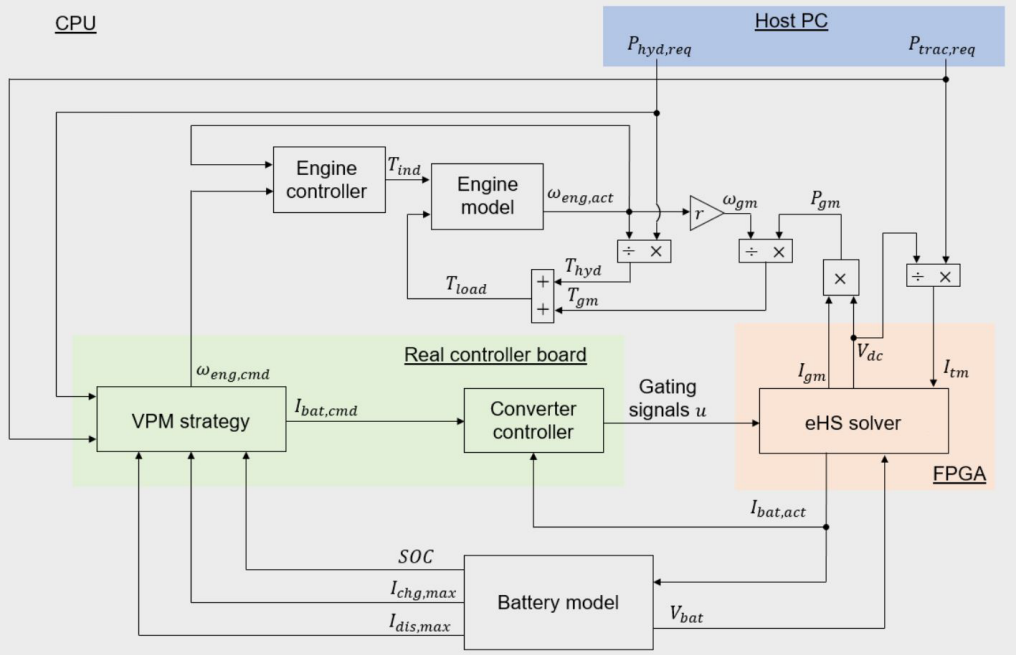

Figure 11. Configuration of HIL simulator setup

Fig. 12 illustrates the concept of replicating a real production drive cycle performed by a baseline vehicle on the HIL simulation platform for the proposed vehicle. Additionally, it also provides an explanation of the procedure for the "Stockpile" drive cycle. It is important to note that when simulating the proposed vehicle on this HIL simulation platform, there is a specific consideration to be addressed. Despite the VPM strategy's ability to direct the engine controller to follow a target engine speed, enabling efficient engine operation, currently the (proposed) demo vehicle assembled by John Deere for ground testing lacks the capability to freely adjust engine speed. Consequently, within the HIL simulation setup, the target engine speed is fixed at 1800 RPM, which is generally an efficient speed for the engine installed in the proposed vehicle.

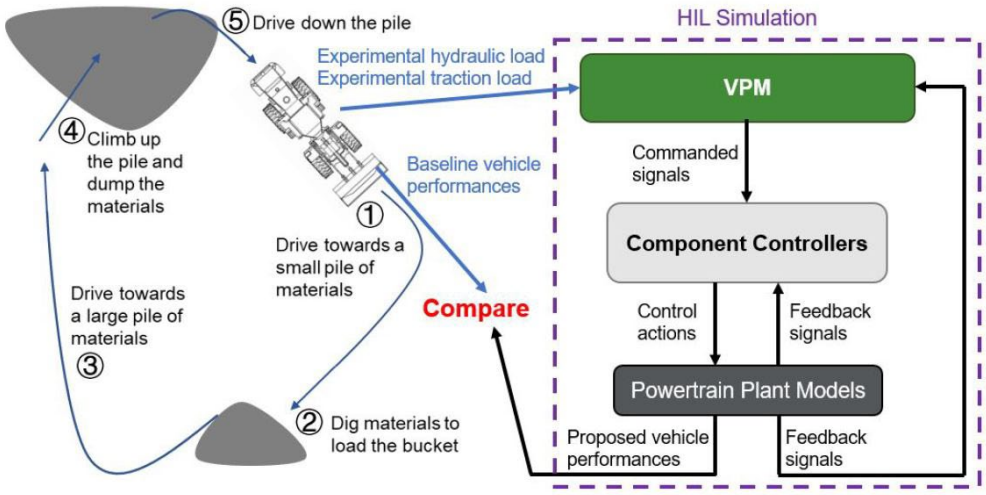

Figure 12. Illustration of reproducing a "Stockpile" drive cycle in the HIL simulator

4.2. Experimental Results

Fig. 13 illustrates the instantaneous power consumption of the two primary power-consuming components on the analyzed wheel loaders as simulated on the HIL platform: the traction motor and hydraulic pump. A positive power value indicates power consumption by the respective unit, while a negative power value indicates power generation by the unit. It is noteworthy that the solid red line represents the actual traction/hydraulic power measured from the baseline vehicle during experimentation, which also serves as the "requested power" inputs ($P_{trac,req}$, $P_{hyd,req}$) for the proposed vehicle (denoted as “Next-gen vehicle” in the figure) in the HIL simulation platform. Meanwhile, the dashed blue line represents the measured simulated traction/hydraulic power delivered by the proposed vehicle in the HIL simulation platform. It is evident that the dashed blue line closely aligns with the solid red line for both power-consuming units across the entire drive cycle. Since traction power signifies vehicle propulsion and hydraulic power indicates the vehicle's bucket operation, this figure leads to the conclusion that despite the proposed wheel loader featuring a downsized engine, it is still capable of delivering equivalent vehicle performance to the baseline wheel loader with the assistance of the battery.

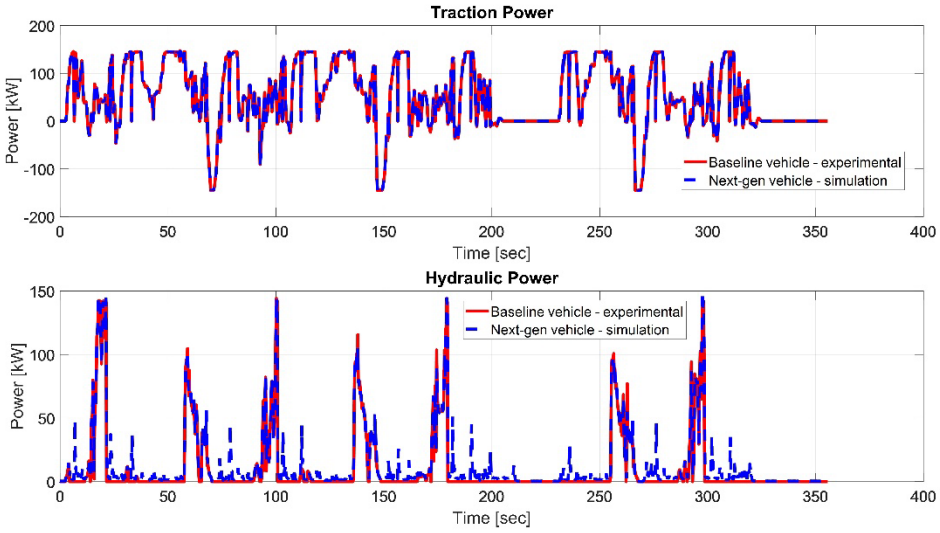

Figure 13. HIL simulation result - power consuming unit performances

Fig. 14 evaluates the performance of the battery in the proposed vehicle during the "Stockpile" drive cycle. The first and second subplots depict the commanded battery power by the VPM strategy, and the actual battery power measured from the plant model, respectively. It is important to note that the commanded battery power is derived from the real controller board, which records simulation results as data points, while the actual battery power is obtained from the CPU module, which records simulation results as time-series data. Consequently, there is not a perfect alignment on the x-axis between the two subplots. However, the two subplots are presented in a manner that reflects correspondence throughout the simulated drive cycle. Analysis of these subplots reveals that the actual battery power closely follows the trend and magnitude of the commanded battery power, notwithstanding some spikes and dips during transients, which are expected. This observation confirms that the DC/DC converter controller effectively regulates the actual battery current in response to commands from the VPM strategy. The third subplot in Fig. 14 illustrates the battery State of Charge (SOC) condition. It is noted that the battery SOC value at the end of the drive cycle matches the initial battery SOC value of 70%, demonstrating that the VPM and component-level control strategies effectively maintain the battery SOC by appropriately discharging and charging the battery without violating its physical limits. Furthermore, the conservation of battery SOC enables a valid comparison between the baseline wheel loader and the proposed wheel loader in terms of engine fuel consumption.

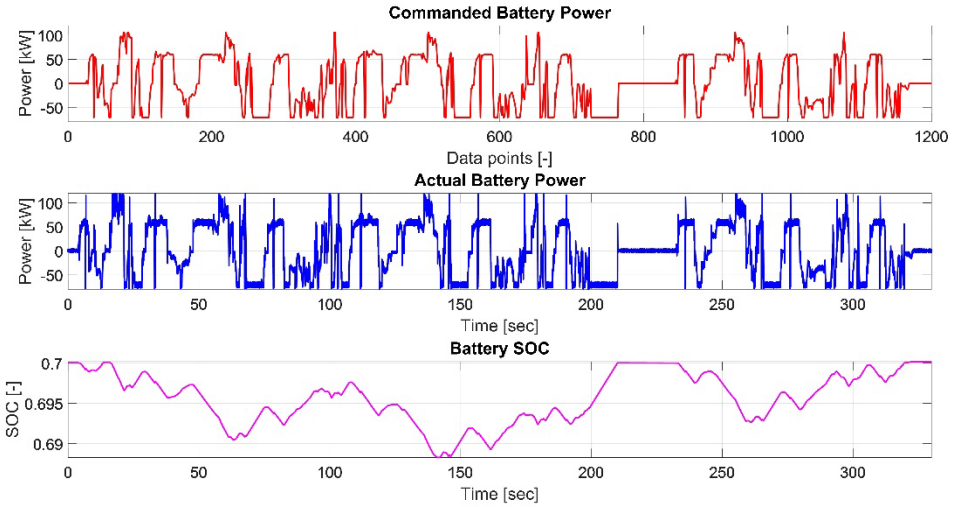

Figure 14. HIL simulation result - battery performances

In Fig. 15, the simulation results of the downsized engine for the proposed hybrid vehicle are analyzed. Similar to the battery, the first two subplots depict the commanded engine power measured from the VPM strategy (in the real controller board) and the actual engine power measured from the engine model (in the CPU module), respectively. It is noteworthy that although engine power is not a direct control variable of the VPM strategy, the close match between actual engine power and commanded engine power throughout the entire drive cycle suggests that the VPM strategy effectively manages power distribution within the proposed hybrid vehicle, without consistently drawing extra power from the engine to compensate for power deficiencies. The third and fourth subplots display engine speed and engine torque, respectively. It is observed that the engine speed controller promptly and accurately regulates the engine speed around 1800 RPM in the simulation, instilling confidence in its deployment on a real controller board for testing the demonstration vehicle. Additionally, it is evident that the commanded engine power remains at 85 kW for the majority of the time, which represents the optimal power level for the engine at 1800 RPM. This insight underscores one of the key objectives of the VPM strategy: to operate the engine efficiently for the purpose of fuel savings.

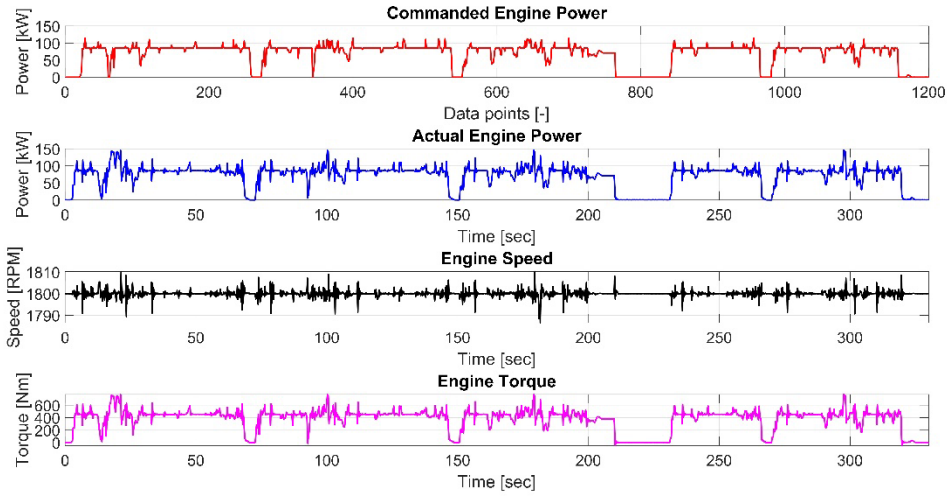

Figure 15. HIL simulation result - engine performances

Fig. 16 examines the fuel consumption of the downsized engine utilized in the proposed vehicle, as depicted by the orange line in both subplots. The top subplot displays the instantaneous engine fueling rate at each time instant. Integrating the instantaneous engine fueling rate over time yields the cumulative engine fuel consumption, which is illustrated in the bottom subplot. For reference, corresponding data of the original engine used in the baseline vehicle are also included, represented by the blue line. It is evident that at the end of the same drive cycle, the original engine of the baseline vehicle consumes 1.82 kg of fuel, whereas the downsized engine of the proposed vehicle consumes only 1.58 kg of fuel, resulting in a 13% fuel saving achieved by the proposed vehicle.

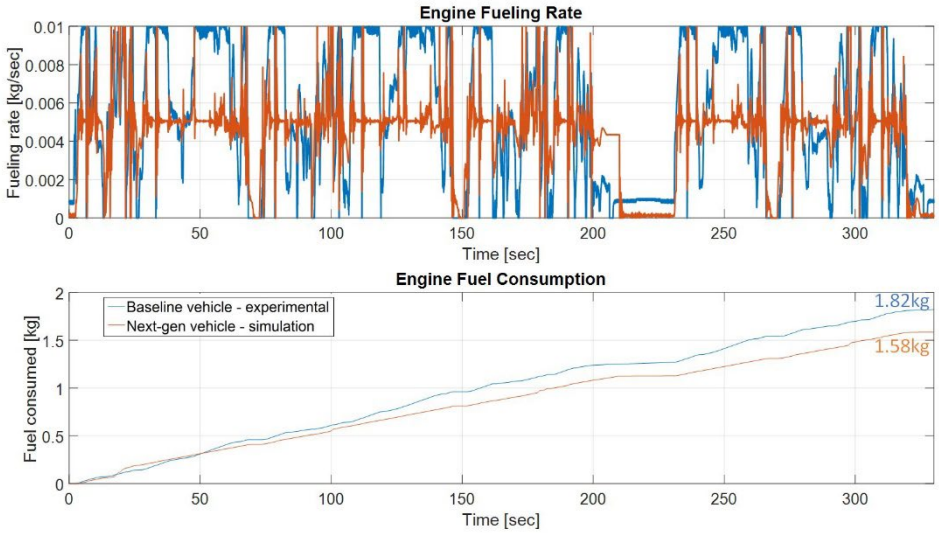

5. CONCLUSIONS

The increasing demand for hybrid wheel loaders in the off-road construction vehicle industry over the past decade is driven by concerns about global warming, rising fuel prices, and stricter government regulations. This heightened demand underscores the necessity for advanced testing methodologies that can facilitate the design of next-generation hybrid wheel loaders. In this research, a cutting-edge hardware-in-the-loop (HIL) simulation platform, comprising a supervisory-level vehicle power management (VPM) strategy, component-level controllers, and vehicle powertrain plant models, has been established for a battery-hybrid wheel loader currently under investigation at John Deere. This HIL simulator enables the safe and efficient real-time validation of an actual controller board that integrates the VPM strategy and a DC/DC converter controller. Additionally, it allows for the evaluation of potential fuel savings achievable with the battery-hybrid wheel loader in comparison to its baseline counterpart.

The results of the HIL simulation demonstrate that the VPM strategy effectively delivers the power demanded by operators from power sources to power consuming units, ensures efficient engine operation, and maintains a balanced battery State of Charge (SOC). Moreover, the ability of the DC/DC converter controller to promptly and accurately regulate battery current to match the target value is confirmed. As a result of engine downsizing and powertrain hybridization, it is anticipated that the proposed battery hybrid electric wheel loader will achieve fuel savings of over 10% in comparison to a baseline wheel loader.

6. REFERENCES

[1] Zhao, Dezong, et al. "Real-time energy management for diesel heavy duty hybrid electric vehicles." IEEE Transactions on Control Systems Technology 23.3 (2014): 829-841.

[2] Fathy, Hosam K., et al. "Review of hardware-in-the-loop simulation and its prospects in the automotive area." Modeling and simulation for military applications. Vol. 6228. SPIE, 2006.

[3] Rayasam, Sree Harsha, et al. "Robust Switching MIMO Control of Turbocharged Lean-Burn Natural Gas Engines." IFAC-PapersOnLine 55.24 (2022): 7-12.

[4] Rayasam, Sree Harsha, et al. "Robust model-based switching MIMO air handling control of turbocharged lean-burn SI natural gas variable speed engines." International Journal of Engine Research 24.6 (2023): 2783-2804.

[5] Qiu, Weijin, et al. "Modeling and Robust Coordinated Control of Turbocharged Natural Gas Engine with Genset Application." IFAC-PapersOnLine 55.24 (2022): 39-44.

[6] Harsha Rayasam, Sree, et al. "Control-oriented modeling, validation, and interaction analysis of turbocharged lean-burn natural gas variable speed engine." International Journal of Engine Research 24.2 (2023): 738-754.

[7] Qiu, Weijin, et al. "Control design-oriented modeling and μ-synthesis-based robust multivariate control of a turbocharged natural gas genset engine." International Journal of Engine Research 24.9 (2023): 3905-3921.

[8] Qiu, Weijin. AN INTEGRATED FRAMEWORK FOR MODELING, ROBUST COORDINATED CONTROL, AND POWER MANAGEMENT OF ADVANCED POWERTRAINS FEATURING TURBOCHARGED ENGINES. Diss. Purdue University Graduate School, 2023.

[9] Qiu, Weijin, et al. "System configuration, control development, and in-field validation of a hybrid electric wheel loader featuring electrically-boosted engine." Control Engineering Practice 150 (2024): 105989.